

OPEN ACCESS

EDITED BY
Jaime Lloret,
Universitat Politècnica de València, Spain

REVIEWED BY
Alejandra Navarro,
Council for Agricultural and Economics
Research (CREA), Italy
Joaquim Bellvert,
Institute of Agrifood Research and
Technology (IRTA), Spain

*CORRESPONDENCE
María R. Conesa
✉ mrconesa@cebas.csic.es

SPECIALTY SECTION
This article was submitted to
Sustainable and Intelligent Phytoprotection,
a section of the journal
Frontiers in Plant Science

RECEIVED 13 December 2022
ACCEPTED 25 January 2023
PUBLISHED 15 February 2023

CITATION
Conesa MR, Conejero W, Vera J and Ruiz-
Sánchez MC (2023) Assessment of trunk
microtensiometer as a novel biosensor to
continuously monitor plant water
status in nectarine trees.
Front. Plant Sci. 14:1123045.
doi: 10.3389/fpls.2023.1123045

COPYRIGHT
© 2023 Conesa, Conejero, Vera and Ruiz-
Sánchez. This is an open-access article
distributed under the terms of the [Creative
Commons Attribution License \(CC BY\)](#). The
use, distribution or reproduction in other
forums is permitted, provided the original
author(s) and the copyright owner(s) are
credited and that the original publication in
this journal is cited, in accordance with
accepted academic practice. No use,
distribution or reproduction is permitted
which does not comply with these terms.

Assessment of trunk microtensiometer as a novel biosensor to continuously monitor plant water status in nectarine trees

María R. Conesa*, Wenceslao Conejero, Juan Vera and M^a Carmen Ruiz-Sánchez

Irrigation Department, Centro de Edafología y Biología Aplicada del Segura (CEBAS-CSIC), Campus de Espinardo, Murcia, Spain

The objective of this work was to validate the trunk water potential (Ψ_{trunk}), using emerged microtensiometer devices, as a potential biosensor to ascertain plant water status in field-grown nectarine trees. During the summer of 2022, trees were subjected to different irrigation protocols based on maximum allowed depletion (MAD), automatically managed by real-time soil water content values measured by capacitance probes. Three percentages of depletion of available soil water (α) were imposed: (i) $\alpha=10\%$ (MAD=27.5%); (ii) $\alpha=50\%$ (MAD=21.5%); and (iii) $\alpha=100\%$, no-irrigation until Ψ_{stem} reached -2.0 MPa. Thereafter, irrigation was recovered to the maximum water requirement of the crop. Seasonal and diurnal patterns of indicators of water status in the soil-plant-atmosphere continuum (SPAC) were characterised, including air and soil water potentials, pressure chamber-derived stem (Ψ_{stem}) and leaf (Ψ_{leaf}) water potentials, and leaf gas exchange, together with Ψ_{trunk} . Continuous measurements of Ψ_{trunk} served as a promising indicator to determine plant water status. There was a strong linear relationship between Ψ_{trunk} vs. Ψ_{stem} ($R^2 = 0.86$, $p < 0.001$), while it was not significant between Ψ_{trunk} vs. Ψ_{leaf} ($R^2 = 0.37$, $p > 0.05$). A mean gradient of 0.3 and 1.8 MPa was observed between Ψ_{trunk} vs. Ψ_{stem} and Ψ_{leaf} , respectively. In addition, Ψ_{trunk} was the best matched to the soil matric potential. The main finding of this work points to the potential use of trunk microtensiometer as a valuable biosensor for monitoring the water status of nectarine trees. Also, trunk water potential agreed with the automated soil-based irrigation protocols implemented.

KEYWORDS

automated irrigation, SPAC, stem water potential, trunk water potential, *Prunus persica* (L)

1 Introduction

World production of peaches and nectarines (*Prunus persica* L. Batsch) has increased steadily over the last decade, ranging from 20.53 to 24.56 million metric tons (Mt) in 2010, and 2020, respectively. China alone accounts for over 45% of world peach and nectarine production, also leading in harvested area. Meanwhile, Spain leads the commercial production of peach and nectarine in the Mediterranean basin (followed by Italy), with an average of 11.58 Mt year⁻¹ in the period 2015–2020 (FAOSTAST, 2022).

Water availability set the upper limit of yield productivity which is the main economic concern for growers worldwide (Feres and Soriano, 2007). Irrigated crops are exposed to different environmental stresses during their growth and development, with drought being the most severe stress that negatively affects plant productivity (Katerji et al., 2008). The effects of drought are aggravated in arid and semi-arid areas, such as the Mediterranean region, due to the alarming depletion of water resources and the increasing demand for food due to population growth (Varela-Ortega et al., 2016; Fernández-García et al., 2020). In addition, the COVID-19 pandemic put a strain on food supply chains worldwide, so urgent and ambitious actions are needed to build more resilient agricultural systems to maximise irrigation water productivity (FAO, 2021).

Drip irrigation is probably the most important and widespread irrigation technique for improving water use efficiency, as it allows optimal use of both water and fertiliser, since they are applied directly to the root system through low-flow emitters (Burt and Styles, 2007). Another advance has been the incorporation of drip irrigation into precise irrigation agriculture, using irrigation scheduling techniques based on monitoring soil and plant water status (Vera et al., 2017; Vera et al., 2019).

Automated irrigation scheduling, based on soil water sensors that provide real-time information, has become a major challenge for precise sustainable irrigation (Vories and Sudduth, 2021). Soil water content (Θ_v) is a state variable often proposed as a key input for irrigation management in decision support systems. Most of the available literature on fruit crops reported automatic irrigation controllers, using Θ_v values with on/off strategies based on real-time feedback protocols, which establish an upper and lower limit of each system state (Casadesús et al., 2012; Romero et al., 2012; Osroosh et al., 2016; Millán et al., 2019; Vories and Sudduth, 2021). In drip-irrigated nectarine trees, threshold Θ_v values converted to

management allowed depletion (MAD) values were proposed to trigger/stop irrigation, thus allowing a more accurate soil-based irrigation scheduling (Vera et al., 2019). In this sense, Conesa et al. (2021) demonstrated that the automated MAD-based irrigation method, combined with regulated deficit irrigation criteria (Ruiz-Sánchez et al., 2010) proved to be a promising method for irrigation scheduling in Mediterranean agrosystems. In fact, precise deficit irrigation based on MAD threshold values used 40% less irrigation volume compared to irrigation based on conventional crop evapotranspiration (ETc) calculations (as the product of crop reference ET by local crop coefficients), maintaining yield and quality of nectarine fruits, and even increasing water use efficiency (Conesa et al., 2019).

Plant-based sensors for water status purposes address the concept of using plants as ‘biosensors’, where soil-water, atmospheric conditions and plant response are integrated (Jones, 2004). Midday stem water potential (Ψ_{stem}) has been accepted worldwide as the most reliable indicator of plant water status (Abriskqueta et al., 2015). Conesa et al. (2019) proposed the long-established Ψ_{stem} as the best reference indicator of the discontinuous plant water status for drip-irrigated nectarine trees. However, Ψ_{stem} is a very labour-demanding and destructive measurement that cannot be automated.

Nowadays, IoT in agriculture has led to the development of many detection methods as plant indicators to measure water status and to assess plant responses to environmental stresses. Indicators of plant water status on a continuous basis include those based on sap flow and stem heat balance (Smith and Allen, 1996; Navarro et al., 2020; Dix and Aubrey, 2021), trunk diameter fluctuations (Fernández and Cuevas, 2010; Ortuño et al., 2010), and leaf turgor (Martínez-Gimeno et al., 2017; Padilla-Díaz et al., 2018). However, although the latter two are non-invasive techniques (Fernández, 2014), the equipment used requires a significant labour input to properly monitor plant water status, as well as specialised staff for data processing.

The emerging sensors identified as microtensiometers (MTs) are embedded in the tree trunk and directly measure the trunk water potential (Ψ_{trunk}) on a continuous basis, which is a major advantage over discrete Ψ_{stem} determinations. This sensor is a microelectromechanical system-based microtensiometer that measures plant water status with a high degree of accuracy. It can be automated and provides easy-to-interpret continuous data, in pressure units comparable to those of the Ψ_{leaf} or Ψ_{stem} acquired with traditional pressure chamber methods (Pagay et al., 2014; Lakso et al., 2022).

To our knowledge, only a few studies have addressed the performance of these MTs sensors in field conditions and under different water availability scenarios (e.g. Blanco and Kalcits (2021) in apple and Pagay (2022) in grapevines). Our hypothesis is that MTs can provide stable continuous Ψ_{trunk} data, and we seek to know if they can be used to validate automated MAD-based irrigation protocols, as we have already done from discrete Ψ_{stem} determinations in previous experiences (Conesa et al., 2019; Vera et al., 2019; Conesa et al., 2021; Mira-García et al., 2021).

This study aims to validate the use of Ψ_{trunk} as a continuous plant-based water status indicator in drip-irrigated nectarine trees grown under Mediterranean conditions threatened by water scarcity. Irrigation scheduling was automatically managed by real-time Θ_v values at different levels of MAD corresponding to well-irrigated,

Abbreviations: Ψ_{air} , air water potential; Ψ_{leaf} , leaf water potential; Ψ_p , leaf osmotic potential; Ψ_{100p} , leaf osmotic potential at full turgor; Ψ_t , leaf turgor potential; Ψ_{trunk} , trunk water potential; Ψ_{stem} , stem water potential; Ψ_m , soil matric potential; MTs, microtensiometers; Θ_v , volumetric soil water content; ET_0 , reference crop evapotranspiration; ET_c , crop evapotranspiration VPD, vapour pressure deficit; SPAC, soil-plant-atmosphere continuum; MAD, maximum allowable depletion; FC, field capacity; WP, wilting point; α , percent depletion of soil available water; P_n , net photosynthesis; g_s , stomatal conductance; E, transpiration rate; WUE_T , transpiration efficiency; DOY, day of the year; GMT, Greenwich mean time. Ψ_{stem} : midday stem water potential (MPa); Ψ_{leaf} : midday leaf water potential (MPa); Ψ_{trunk} : midday trunk water potential (MPa); P_n : net photosynthesis ($\mu\text{mol m}^{-2} \text{s}^{-1}$); g_s : stomatal conductance ($\text{mmol m}^{-2} \text{s}^{-1}$); WUE_T : transpiration efficiency ($\mu\text{mol mmol}^{-1}$).

moderate deficit and drought conditions. The performance of MAD-based irrigation method was also analysed in the soil-plant-atmosphere continuum

2 Material and methods

2.1 Field conditions

The experiment was carried out from June to September in 2022, in a 0.5 ha orchard of twelve-year-old early-maturing nectarine trees (*Prunus persica* (L.) Batsch, cv. Flariba, on GxN-15 rootstock), at the CEBAS-CSIC experimental station, Murcia (Spain, 38° 06' 31" N, 1° 02' 14" W). The trees were spaced 6.5 m x 3.5 m and trained to an open-centre canopy. The soil in the 0-0.5 m layer was stony and shallow with a clay-loam texture and low organic matter content 1.3%. The average bulk density was 1.43 g cm⁻³. Soil water content (Θ_v) at field capacity and at permanent wilting point was 0.29 and 0.14 m³ m⁻³, respectively. The drip-irrigation system consisted of one dripline per row of trees with four pressure-compensated emitters (4 l h⁻¹) per tree located 0.5 and 1.3 m from the tree trunk. The amount of water applied was measured with a pulse flowmeter (Sensus, 120 HRI-A, Barcelona, Spain).

Seasonal fertiliser applications were 83, 56, and 109 kg ha⁻¹ of N, P₂O₅ and K₂O, respectively, applied by fertigation system (Vera and de la Peña, 1994). Other usual cultural practices (e.g. weed control, fertilization, pruning, fruit thinning) were carried out following the recommendations of commercial fruit tree orchards.

The experiment consisted of an automated soil-based irrigation treatment, managed according to different irrigation criteria (see 2.4 section), which were randomly distributed in four replicates, each consisting of six nectarine trees (n= 24). Measurements of soil and plant water relations were taken on a representative tree from each replicate.

2.2 Agrometeorological status

During the experimental period, agrometeorological data (air temperature, T_a; relative humidity, RH; and rainfall) were recorded every 15 min by an automatic weather station located in the CEBAS-CSIC experimental field, next to the nectarine tree orchard (http://www.cebas.csic.es/general_spain/est_meteo.html). Hourly reference crop evapotranspiration (ET₀, mm) was calculated following the Penman-Monteith equation (Allen et al., 1998). Vapour pressure deficit (VPD, kPa) was calculated from daily maximum T_a and minimum RH.

The hourly air water potential ($\Psi_{air,MPa}$) was calculated with the equation (Nobel, 1983):

$$\Psi_{air} = \frac{R \cdot T}{V_w} \ln \frac{RH}{100} \quad (1)$$

where, R is the gas constant (R=0.082 atm L K⁻¹ mol⁻¹), T is the absolute temperature (273+T_a, °C), V_w the partial molar volume of water in the atmosphere (18 cm³ at 20 °C), and RH is the air relative humidity (%).

2.3 Soil water status

Soil water status was continuously monitored by measurements of soil water content (Θ_v) and soil matric potential (Ψ_m), as follows:

2.3.1 Soil water content

Volumetric soil water content (Θ_v , %) was monitored with multi-depth EnviroScan[®] capacitance probes (Sentek Sensor Technologies, Sidney, Australia). Four PVC access tubes were installed 10 cm from the emitter located close (0.5 m) to the tree trunk in four representative trees (one in each replicate). Each capacitance probe had sensors at 0.1, 0.3, 0.5, and 0.7 m depth, and was connected to a radio transmission unit. Values were read every 5 min and the average was recorded every 15 min. The probes were normalised and calibrated following the procedure proposed by Starr and Paltineanu (2002). Drip gauges (Pronamic, Ringkoebing, Denmark) were installed below the emitter near the capacitance probe to monitor real-time irrigation amounts and to detect any flow rate failures during the irrigation events. The radio-transmission units sent the data to a gateway that is connected to the addVANTAGE cloud server (ADCON Telemetry, Vienna, Austria) for data acquisition, processing, and visualisation.

2.3.2 Soil matric potential

Soil matric potential (Ψ_m , kPa) was measured with digital tensiometers (WEENAT, Nantes, France) consisting of granular matrix sensors, which were installed in the wet bulb of two nectarine trees, at 0.3 and 0.6 m soil depth. Data were recorded and visualised on the cloud platform www.weenat.com.

2.4 MAD-based irrigation protocol

Average Θ_v values of the 0-0.5 m soil profile, representing the active water uptake of the roots (Abrisqueta et al., 2017), were used to act on electro-valves by means of the telemetry network (see 2.3.1 section). The maximum allowable depletion (MAD) values were established as irrigation threshold Θ_v , as derived from the concept proposed by Merriam (1966), as:

$$MAD = FC - \alpha \frac{(FC - WP)}{100} \quad (2)$$

where, FC is the field capacity, WP is the wilting point, α is the percentage depletion of available water in the soil.

In the experiment, the following α criteria were applied:

α = 10%: well-irrigated, from 3 to 29 June 2022.

α = 50%: moderate soil water deficit, from 30 June to 29 July 2022.

α = 100%: severe soil water deficit. No irrigation was applied from 30 July to 1 September 2022.

Recovery: Irrigation recovered at full crop water requirements, when Ψ_{stem} reached -2.0 MPa, from 2 September to 30 September 2022.

2.5 Plant water status

During the experimental period, plant water status was estimated by weekly measurements of discrete plant-based water indicators: leaf and stem water potentials and leaf gas exchange. In addition, daily time-courses were made on representative days of the well-irrigated period (23 June 2022, DOY 174), at the end of the moderate water deficit ($\alpha=50\%$) period (29 July 2022, DOY 210), and at the end of drought ($\alpha=100\%$) period (1 September 2022, DOY 244). All measurements were always performed on one leaf of the same trees in each replicate ($n=4$). In addition, trunk water potential was measured continuously in two of the four replicates ($n=2$).

2.5.1 Leaf and stem water potentials

Leaf (Ψ_{leaf} , MPa) and stem (Ψ_{stem} , MPa) water potentials were measured on four leaves (one leaf per replication) at midday (13:00–14:00 h, GMT+2), and hourly during daily courses on fully expanded healthy leaves, using a pressure chamber (Soil Moisture Equipment Corp. Model 3000, Santa Bárbara, CA, USA) as recommended by Turner (1988). Measurements of Ψ_{leaf} were made in sunny, freely transpiring leaves, while for Ψ_{stem} , leaves were located on the shaded side of the tree, close to the tree trunk, and covered with aluminium foil for at least 2 h before the determinations (McCutchan and Shackel, 1992). Both measurements were carried out weekly during the experiment, as well as hourly in the daily time-courses.

2.5.2 Trunk water potential

Trunk water potential (Ψ_{trunk} , MPa) was determined using microtensiometers (MTs; FloraPulse, Davis, CA, USA, www.florapulse.com) embedded directly into the trunk on the shaded side of two nectarine trees, at 0.4 m from soil surface (Illustration 1A). Installation of the MTs was carried out according to the recommendations of the manufacturer. The technical details given by Pagay et al. (2014); Black et al. (2020), and Lakso et al. (2022) were also considered. The sensors were allowed to equilibrate with the tree (through the mating compound) within 2 days of installation (Pagay, 2022). Trunk water potential (Ψ_{trunk}) data were obtained every 15 min, and transmitted using the same telemetry network (ADCON Telemetry, Vienna, Austria) (Illustration 1B).

2.5.3 Leaf osmotic potentials

Leaf osmotic potentials (Ψ_{π} , MPa) were determined at predawn, midday and afternoon on the same leaves used for Ψ_{leaf} determinations, coinciding with daily time-courses. Leaves were frozen in liquid nitrogen and the osmotic potential was measured after thawing the samples and expressing sap by using a vapour pressure osmometer (model WESCOR-5520; Wescor Inc., Logan, UT, USA) following the recommendations of Gucci et al. (1991). Leaf turgor potentials (Ψ_t , MPa) at predawn, midday and afternoon were calculated as the difference between osmotic and leaf water potentials. Leaf osmotic potential at full turgor ($\Psi_{\pi100}$, MPa) was measured on leaves adjacent to those used for Ψ_{leaf} at predawn. The leaves were excised and placed by their petioles in distilled water overnight to reach full saturation, after which they were frozen in liquid nitrogen ($-196\text{ }^{\circ}\text{C}$) and stored at $-30\text{ }^{\circ}\text{C}$, following the same methodology as for Ψ_{π} . The osmotic adjustment was estimated by comparing $\Psi_{\pi100}$ values at $\alpha=10\%$ (well-irrigated), and $\alpha=100\%$ (non-irrigated).

2.5.4 Leaf gas exchange

Net photosynthesis (P_n , $\mu\text{mol m}^{-2}\text{ s}^{-1}$), stomatal conductance (g_s , $\text{mmol m}^{-2}\text{ s}^{-1}$), and transpiration rate (E , $\text{mmol m}^{-2}\text{ s}^{-1}$) were measured on one mature sunny leaf per replication ($n=4$) in the early morning (9:00–10:00 h, GMT+2), using a portable gas exchange system (LI-COR, LI-6400) at photon flux density (PPFD) $\approx 1500\text{ }\mu\text{mol m}^{-2}\text{ s}^{-1}$ and CO_2 concentration $\approx 400\text{ }\mu\text{mol mol}^{-1}$. During daily time-courses, hourly leaf gas exchange measurements were taken under ambient PPFD conditions at the time of measurements. Transpiration efficiency (WUE_T , $\mu\text{mol mmol}^{-1}$) was calculated as the P_n/E ratio.

2.6 Sensitivity analysis

For the plant-based status indicators, the signal intensity (SI) was calculated as the ratio between all data registered at $\alpha=100\%$ (drought conditions) and $\alpha=10\%$ (well-irrigated conditions) periods. To determine noise, the coefficient of variation (CV) of the measurements was calculated for each indicator.

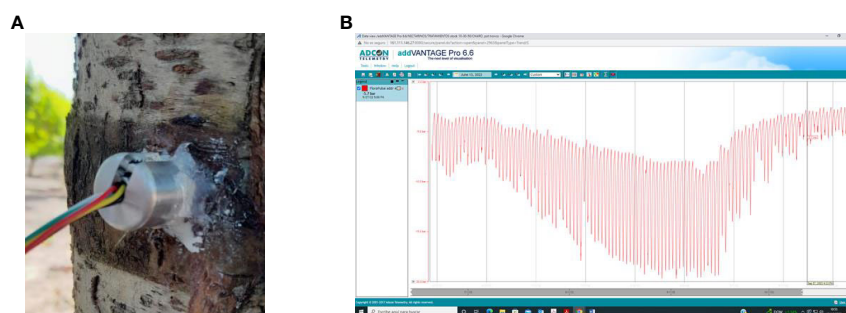


ILLUSTRATION 1

(A) MT sensor installed in the nectarine tree trunk, and (B) data visualisation of Ψ_{trunk} on addVANTAGE web server.

Sensitivity was determined using two algorithms:

- Traditional method (S), as proposed by Goldhamer and Fereres (2001):

$$S = \frac{SI}{CV} \tag{3}$$

S is always greater than 0, and the higher the value, the greater the sensitivity.

- Corrected sensitivity (S*), as proposed by De la Rosa et al. (2014).

$$S^* = \frac{(SI - 1)}{CV} \tag{4}$$

The interpretation of the values obtained with this algorithm is as follows:

- (a) $S^* > 1$: indicates sensitivity to water deficit.
- (b) $1 > S^* > 0$: The noise is greater than the increase in signal intensity.
- (c) $S^* = 0$: not sensitive to water deficit.
- (d) $S^* < 0$: anomalous behavior.

2.7 Statistical analysis

Data were depicted using the SigmaPlot v. 14.5 software (Inpixon, PA, USA). Statistical comparisons were considered significant at $p < 0.05$, using Pearson's correlation coefficient. Relationships between indicators of plant and soil water status were explored by linear regression analyses. The coefficient of determination (R^2) and mean squared error (MSE) were used to assess the goodness of fit. All analyses were performed with SPSS v. 9.1 (IBM, Armonk, NY, USA).

3 Results

3.1 Automated control of irrigation and climatology

The climatic conditions during the experiment, comprising the postharvest period of the early-maturing nectarine trees (June to October), corresponded to a typical Mediterranean semi-arid summer environment, high values of ET_0 (472.1 mm) and low rainfall (10.2 mm concentrated during the recovery period). Daily VPD values varied in a range of 0.2 and 3.3 kPa, representing the greatest day-to-day variability of the agrometeorological variables studied (Figure 1A).

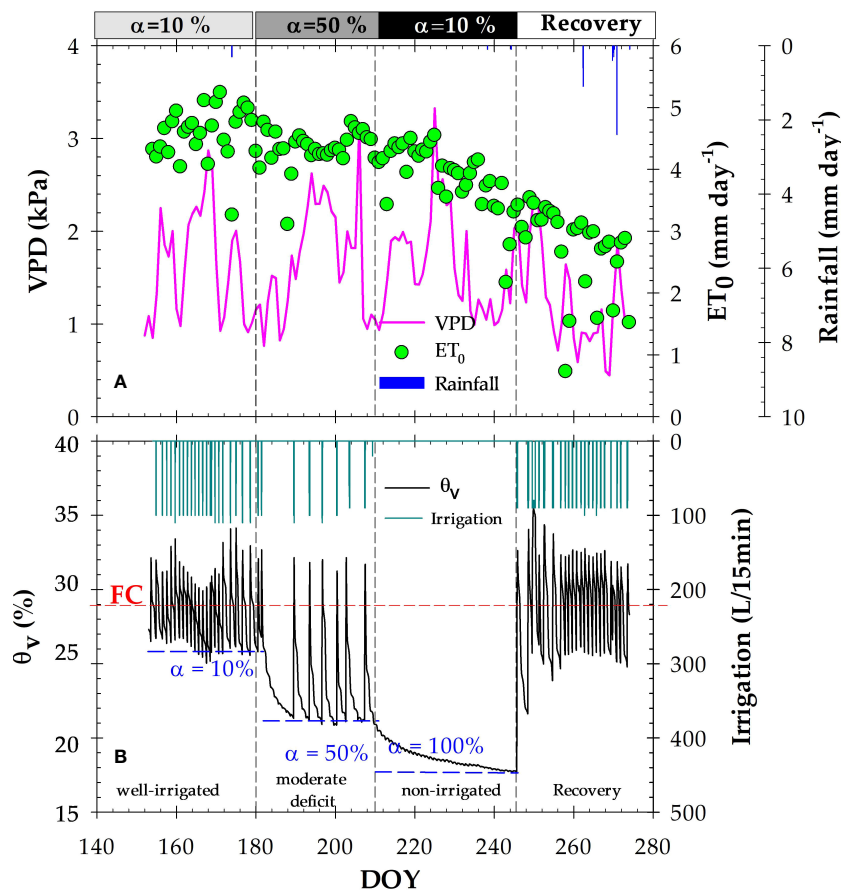


FIGURE 1
(A) Daily vapour pressure deficit (VPD, kPa), reference crop evapotranspiration (ET_0 , mm), and rainfall (mm); **(B)** Soil water content (θ_v , %) in the 0–0.5 m soil profile, and irrigation events (mm), during the experimental period. The dashed horizontal red line corresponds to the field capacity (FC), and the dashed blue lines indicate the soil water deficit (α) criteria: 10% (well-irrigated), 50% (moderate deficit) and 100% (severe deficit, non-irrigated), respectively. The dashed vertical lines delimit each irrigation criterion. DOY: Day of the year.

Volumetric soil water content (Θ_v) fluctuated in response to irrigation, root water uptake and rainfall events. Furthermore, Θ_v in the active root zone (0-0.5 m depth) was clearly influenced by the different imposed MAD-based protocols (Figure 1B). At $\alpha=10\%$, MAD=27.5% (well-irrigated conditions) induced by daily irrigation frequency, Θ_v values varied around field capacity (FC), increasing slightly above this value at the end of each irrigation event. At $\alpha=50\%$, MAD=21.5% (moderate soil water deficit) induced an irrigation frequency of 2 or 3 day. When irrigation water was withheld ($\alpha=100\%$), Θ_v decreased until the minimum value of $\Theta_v \approx 17\%$, close to the wilting point value. Subsequently, during the recovery

period, Θ_v reached variable FC values in response to irrigation and, to a lesser extent, rainfall events. The total amount of irrigation applied during the experiment (including the recovery phase) was 109.5 mm (Figure 1B).

3.2 Seasonal soil-plant-atmosphere water indicators

The data in Figure 2 show the seasonal course of water status in the soil-plant-atmosphere continuum (SPAC). The seasonal trend of

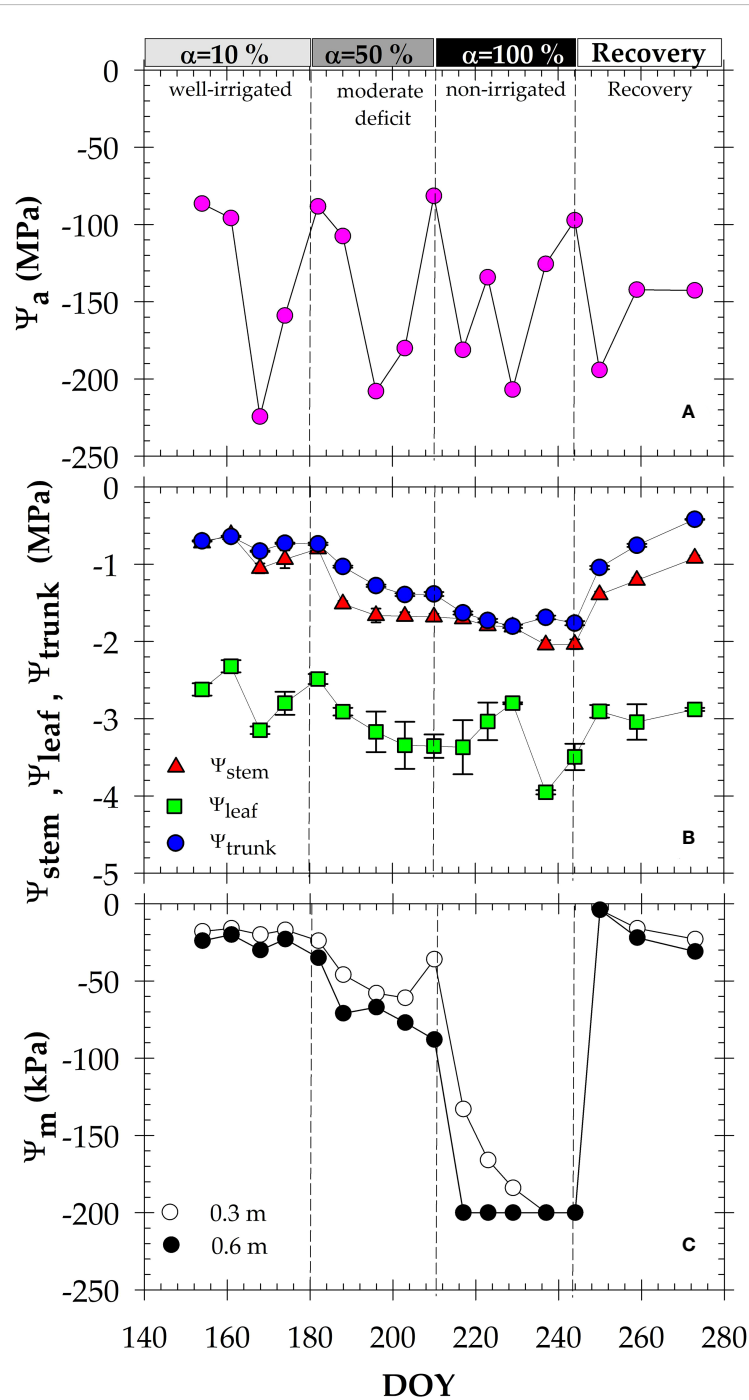


FIGURE 2
 Seasonal course of: (A) daily mean air water potential (Ψ_{air}); (B) midday stem (Ψ_{stem}), leaf (Ψ_{leaf}) and trunk (Ψ_{trunk}) water potentials, and (C) soil matric potential (Ψ_m) at 0.3 and 0.6 m of the soil profile. Each point is the average of four leaves, two MTs, and two granular matrix sensors. Vertical bars at data points are \pm SE (not shown when smaller than the symbols). Dashed vertical lines delimit each irrigation criterion. DOY: Day of the year.

air water potential (Ψ_{air}) was highly variable from day-to-day during the study, with a maximum value of -81.5 MPa (DOY 210, $\alpha=50\%$) and minimum of -224 MPa (DOY 168, $\alpha=10\%$) (Figure 2A).

Soil water potential from the granular matrix sensors (Ψ_m), assuming osmotic and gravitational components to be negligible, ranged from -4 ± 0.85 to -26 ± 1.26 kPa at both depths explored (0.3 and 0.6 m) under well-irrigated conditions ($\alpha=10\%$). Under moderate deficit conditions ($\alpha=50\%$), Ψ_m decreased, showing slightly lower values at 0.6 than at 0.3 m, and reaching minimum values of -61 ± 3.45 and -77 ± 4.48 kPa (MPa) at 0.3 and 0.6 m, respectively. When irrigation was suspended ($\alpha=100\%$), Ψ_m continued to decrease, reaching its minimum allowable reading (-200 kPa) only one week later at 0.6 m depth, and after 13 days of withholding irrigation at 0.3 m (Figure 2C).

Plant water potentials evaluated at three canopy levels (leaf, stem and trunk) reflected the different MAD applied during the experiment (Figures 2A, B). Both Ψ_{stem} and Ψ_{trunk} exhibited a constant pattern during $\alpha=10\%$, averaging -0.83 ± 0.09 and -0.73 ± 0.06 MPa, respectively, during this well-irrigated period. In accordance with the imposed soil water deficit, the trend of both plant indicators decreased, reaching the minimum values of $\Psi_{stem} = -2.04 \pm 0.06$ MPa and $\Psi_{trunk} = -1.81 \pm 0.29$ MPa, at the end of $\alpha=100\%$. A more irregular trend was observed for Ψ_{leaf} during the experiment, showing lower values than those of Ψ_{stem} and Ψ_{trunk} , and minimum values of -3.95 ± 0.26 MPa at the end of the irrigation withholding phase (DOY 237, $\alpha=100\%$).

Correlation analysis between soil and plant water potentials showed a close linear relationship with the highest dependence found between Ψ_m and Ψ_{trunk} ($R^2 = 0.79$), and the lowest (not significant) between Ψ_m and Ψ_{leaf} ($R^2 = 0.26$) (Figure 3). However, there was no significant correlation between Ψ_{air} and plant water potentials (data not shown).

During the experiment, the gradient between midday values of Ψ_{stem} and Ψ_{trunk} varied over a range of 0.02 to 0.5 MPa, while this gradient was higher for Ψ_{leaf} and Ψ_{trunk} (1.0 to 2.5 MPa) (Figure 2B). In this regard, Ψ_{trunk} data obtained with microtensiometers (MTs) were correlated with the plant-based indicators measured with a pressure chamber: Ψ_{stem} and Ψ_{leaf} (Figure 4). The results indicated a

robust significant correlation between Ψ_{trunk} to Ψ_{stem} ($R^2 = 0.86$), and, again, to a lesser extent between Ψ_{trunk} to Ψ_{leaf} ($R^2 = 0.37$).

Leaf gas exchange (P_n and g_s), measured simultaneously with stem and leaf water potentials, showed a seasonal trend that mirrored the soil deficit imposed by the MAD-irrigation protocols (Figures 5A, B). At $\alpha=10\%$, both P_n and g_s reached their maximum values of about $22 \pm 0.34 \mu\text{mol m}^{-2} \text{s}^{-1}$ and $320 \pm 30.5 \text{ mmol m}^{-2} \text{s}^{-1}$, respectively. The lowest values of P_n ($8.6 \pm 0.51 \mu\text{mol m}^{-2} \text{s}^{-1}$) and g_s ($63.5 \pm 9.05 \text{ mmol m}^{-2} \text{s}^{-1}$) were obtained at the end of the $\alpha=100\%$ period (severe water deficit). P_n and g_s also varied in response to plant water potentials under quite contrasting environmental conditions (Figure 2B). Values of WUE_T increased with the imposed soil water deficit (Figure 5C), reaching a maximum value of $5.5 \pm 0.10 \mu\text{mol mmol}^{-1}$. (Figures 5C). It is also important to note that despite irrigation being re-established during the recovery phase, the mean values of P_n and g_s were lower than those obtained under well-irrigated conditions ($\alpha=10\%$).

3.3 Diurnal indicators of soil-plant-atmosphere water status

The daily time-course of soil-plant-atmosphere water status indicators were evaluated on representative days of the well irrigated period (23 June 2022, DOY=174), at the end of moderate water deficit ($\alpha=50\%$) period (29 July 2022, DOY=210), and at the end of drought ($\alpha=100\%$) period (1 September 2022, DOY=244) covering the whole daily light period (06:00 to 21:00 h). The values of soil water content during well irrigated period were 27.82 ± 0.49 ; 39.54 ± 0.35 ; 26.63 ± 0.28 and $33.50 \pm 0.19\%$ at 0.1, 0.3, 0.5, and 0.7 m of soil depth, respectively. Meanwhile, at $\alpha=50\%$, and $\alpha=100\%$, θ_v decreased up to 35% below the FC values, mainly affecting the upper soil depth (> 0.5 m) with little variation observed at the deeper layer (data not shown). In addition, Ψ_m remained constant during each daily course, decreasing as water deficit increased (Figures 6G–I).

Agrometeorological conditions changed greatly during the days selected for punctual measurements (Figures 6A–C). A very demanding day coincided with the well-irrigated period ($\alpha=10\%$), being the warmest of the three diurnal courses studied, with

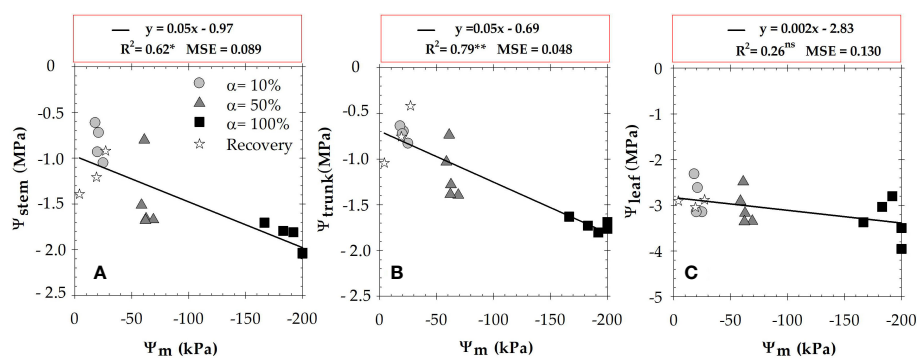


FIGURE 3 Relationship between the midday values of soil matric potential (Ψ_m) (average of 0.3 and 0.6 m), and (A) stem water potential (Ψ_{stem}); (B) trunk water potential (Ψ_{trunk}); and (C) leaf water potential (Ψ_{leaf}), during the experimental period. The different symbols correspond to the four irrigation criteria. Each point is the mean of four leaves and two matrix sensors. R^2 is the coefficient of determination. *: $p \leq 0.05$ **: $p \leq 0.01$, ns: not significant. MSE: mean squared error.

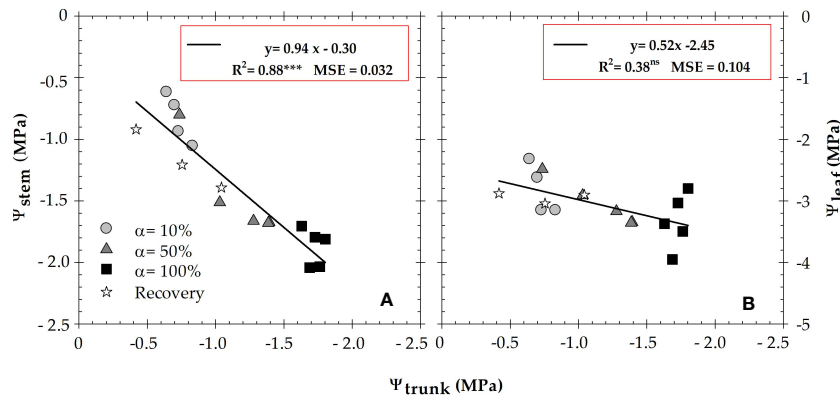


FIGURE 4
 Relationship between midday values of trunk water potential (Ψ_{trunk}) and (A) stem water potential (Ψ_{stem}), and (B) leaf water potential (Ψ_{leaf}), during the experimental period. The different symbols correspond to the different irrigation criteria. Each point is the mean of four leaves and two matrix sensors. R^2 is the coefficient of determination. ***: $p \leq 0.001$, ns: not significant. MSE: mean squared error.

minimum Ψ_{air} values of -218 MPa registered in the early afternoon. Sunny mild-demanding days corresponded to the end of $\alpha=50\%$ and $\alpha=100\%$ periods, when minimum Ψ_{air} values of -84 and -124 MPa were recorded at midday, respectively.

The diurnal patterns of plant water potentials mirrored the imposed soil water deficit based on MAD-threshold values (Figures 6D–F), despite the different climatic conditions observed. At $\alpha=10\%$, minimum values of -0.87 ± 0.08 , -1.30 ± 0.06 and -2.1 ± 0.31 MPa were measured in the early afternoon (16:00 h GMT+2) for Ψ_{trunk} , Ψ_{stem} , and Ψ_{leaf} , respectively. At $\alpha=50\%$, plant water potentials recorded their minimum values at different times of the day. In this sense, Ψ_{leaf} and Ψ_{stem} obtained their minimum values at midday: -3.3 ± 0.26 MPa (Ψ_{leaf}) and -1.8 ± 0.12 MPa (Ψ_{stem}), whereas the minimum value of Ψ_{trunk} (-1.6 ± 0.19 MPa) was obtained in the afternoon (17:00 GMT+2). The severe water deficit situation recorded at $\alpha=100\%$ induced a decrease in plant water potentials from predawn onwards. In this period, Ψ_{leaf} and Ψ_{stem} reached again their minimum values at midday (-3.5 ± 0.26 , and -2.1 ± 0.12 MPa, respectively); and those for Ψ_{trunk} (-1.9 ± 0.21 MPa) in the afternoon (17:00 GMT+2) (Figures 6D–F). It must be emphasized that the values of water potentials at predawn decreased from -0.35 ± 0.08 , -0.68 ± 0.03 to -0.80 ± 0.11 MPa, at $\alpha=10$, 50, and 100% periods, respectively.

To represent the SPAC resistances to water flow along the soil-plant-atmosphere continuum, the experimental values of water potentials at midday were drawn (Figure 7). It can be observed that the highest gradient was found from leaf to air, which is tuned by stomatal aperture, regulating the change of water state from liquid to gas, while the lowest gradient (0.3 MPa) was between Ψ_{trunk} and Ψ_{stem} . Under well irrigated conditions, the next important gradient was between Ψ_{stem} and Ψ_{leaf} (1.7 MPa), followed by Ψ_{m} to Ψ_{trunk} gradient (0.7). As the water deficit progresses, these gradients increase, especially in the case of root to trunk water potential differences (1.5 MPa at the end of the non-irrigation period), and remained almost constant for Ψ_{stem} to Ψ_{leaf} gradient, and even decreased for leaf to air water potentials.

The data in Figure 8 illustrates the diurnal variations of the relationship of Ψ_{trunk} with Ψ_{stem} (A) and Ψ_{leaf} (B) at the different irrigation periods. Notably, values of Ψ_{trunk} in the early afternoon

recovered their morning values at higher Ψ_{stem} values (Figure 8A). This fact was more noticeable when considering Ψ_{leaf} values (Figure 8B). The significance of the coefficient of determinations was higher during the well irrigated period, and decreased at $\alpha=50\%$, not being significant at $\alpha=100\%$ (Figures 8A, B).

Regarding daily leaf gas exchange courses, P_n and g_s increased from sunrise at 08:00 h to 10:30 h GMT+2, which was the period of maximum photosynthetic efficiency in all irrigation conditions studied (Figure 9). During midday, leaf gas exchange exhibited a decrease in its values, although it corresponded with the peaks of solar radiation (R_s) (Figures 9A–C). In the afternoon from 16:00 h to 18:00 h GMT+2, leaf gas exchange parameters exhibited a slightly recovery, even under water deficit conditions ($\alpha=50$ and 100%). From that moment on, the course of leaf gas exchange parameters tended to decrease, until the night hours when minimum values were recorded.

The diurnal patterns of leaf gas exchange followed the established MAD values (Figures 1B, 9). In this sense, at $\alpha=10\%$, the values corresponded to well-irrigated conditions, with maximum values of $17.12 \pm 0.65 \mu\text{mol m}^{-2} \text{s}^{-1}$, $308 \pm 32.9 \mu\text{mol m}^{-2} \text{s}^{-1}$ and $5.54 \pm 0.35 \text{mmol mmol}^{-1}$, for P_n , g_s and WUE_T , respectively. As expected, the lowest values were obtained under severe water deficit situation ($\alpha=100\%$), with maximum daily values of $P_n = 10.94 \pm 0.60 \mu\text{mol m}^{-2} \text{s}^{-1}$, $g_s = 137.1 \pm 8.60 \mu\text{mol m}^{-2} \text{s}^{-1}$ and $\text{WUE}_T = 4.04 \pm 0.08 \text{mmol mmol}^{-1}$.

3.4 Osmotic water potentials

Figure 10 shows the values of osmotic water potential (Ψ_{π}) determined at different times (predawn, midday and afternoon) during the diurnal courses of the different irrigation criteria. At $\alpha=10\%$ (well-irrigated), Ψ_{π} significantly increased from -1.61 ± 0.01 MPa at predawn to -2.97 ± 0.01 MPa in the afternoon. Under water deficit conditions, the minimum Ψ_{π} was found at midday, with values of -3.14 ± 0.05 MPa (at $\alpha=50\%$) and -3.10 ± 0.10 MPa (at $\alpha=100\%$) (Figure 10A). In contrast, the osmotic potential at full turgor ($\Psi_{\pi 100}$) measured at predawn was similar throughout the experimental period with a mean value of -1.76 ± 0.03 MPa (Figure 10A).

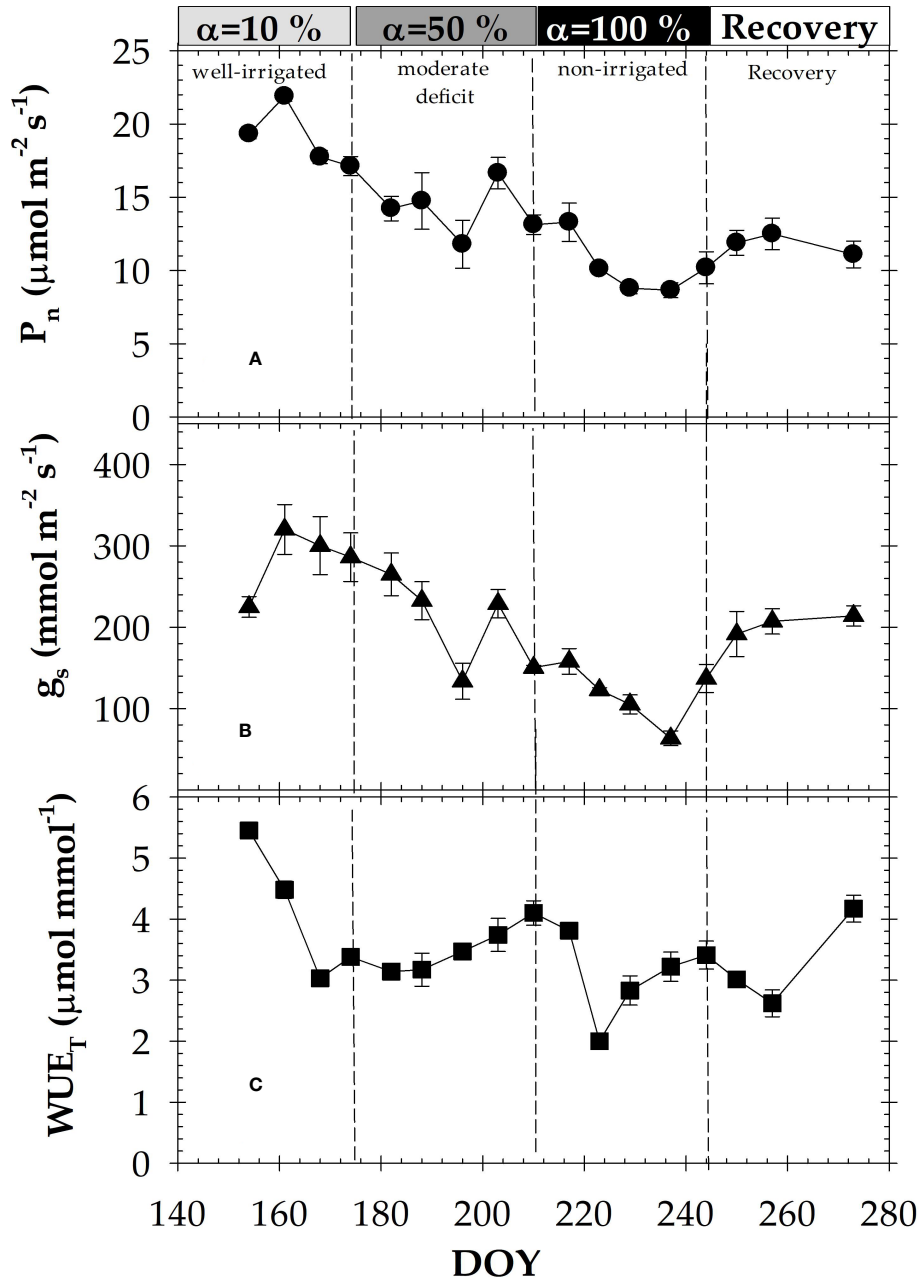


FIGURE 5
 Seasonal time-course of: (A) net photosynthesis (P_n); (B) stomatal conductance (g_s); and (C) transpiration efficiency (WUE_T) during the experimental period. Each point is the mean of four leaves. Vertical bars in data points are \pm SE (not shown when smaller than the symbols). Dashed vertical lines delimit each irrigation criterion. DOY: Day of the year.

The leaf turgor potential (Ψ_t) decreased close to zero as soil water deficit increased (Figure 10B). In this sense, at $\alpha=100\%$ lower Ψ_t values were computed at midday coinciding with the lower leaf water potential (Ψ_{leaf}) and higher evaporative demand values (Figure 6).

3.5 Sensitivity analysis

Comparative analysis of the sensitivity of the indicators of plant water status revealed that plant water potentials showed a higher sensitivity than those obtained for leaf gas exchange (Table 1). From the plant water potentials: Ψ_{trunk} , Ψ_{stem} and Ψ_{leaf} , it was clear that

Ψ_{trunk} was clearly the plant-based water status indicator with the highest SI and sensitivity values by the two methods assessed (S and S^*), followed by Ψ_{stem} and to a lesser extent by Ψ_{leaf} and leaf gas exchange parameters (Table 1). In particular, CV was slightly lower for Ψ_{stem} (2.15) than for Ψ_{trunk} (2.47). The S was similar between Ψ_{trunk} and Ψ_{stem} , even though S^* indicated a higher sensitivity for Ψ_{trunk} .

4 Discussion

Continuous recording of trunk water potential (Ψ_{trunk}) obtained *in situ* with MTs has been a suitable measure of plant water status of

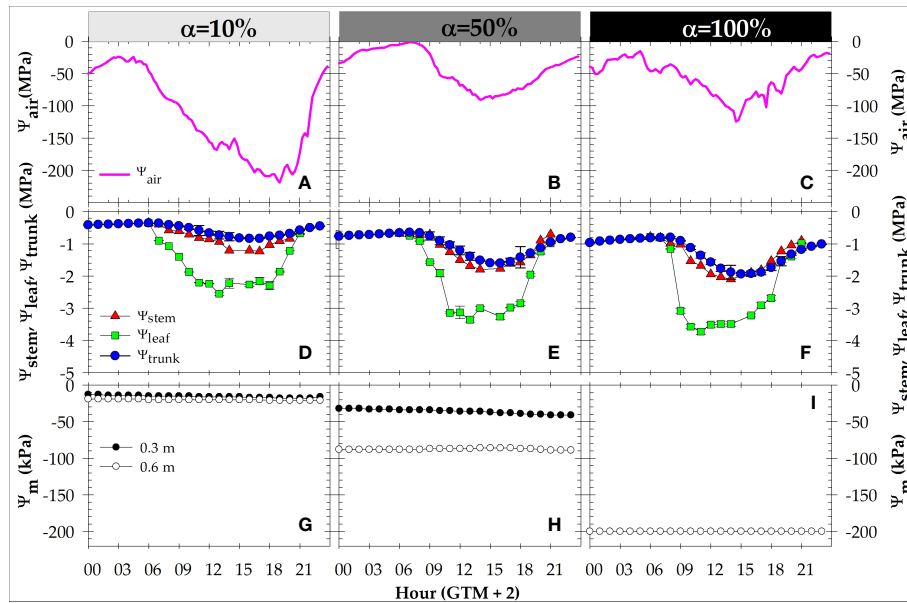


FIGURE 6
 Daily time-courses of: (A-C) air water potential (Ψ_{air}); (D-F) leaf (Ψ_{leaf}), stem (Ψ_{stem}), and trunk (Ψ_{trunk}) water potentials; and (G-I) soil matric potential (Ψ_m) at 0.3 and 0.6 m in the soil profile, during different irrigation criteria: $\alpha=10\%$ (DOY 174), $\alpha=50\%$ (DOY 210) and $\alpha=100\%$ (DOY 244). Each point is the mean of four leaves, two MTs, and two granular matrix sensors. Vertical bars in the data points are \pm SE (not shown when smaller than the symbols). GMT: Greenwich mean time.

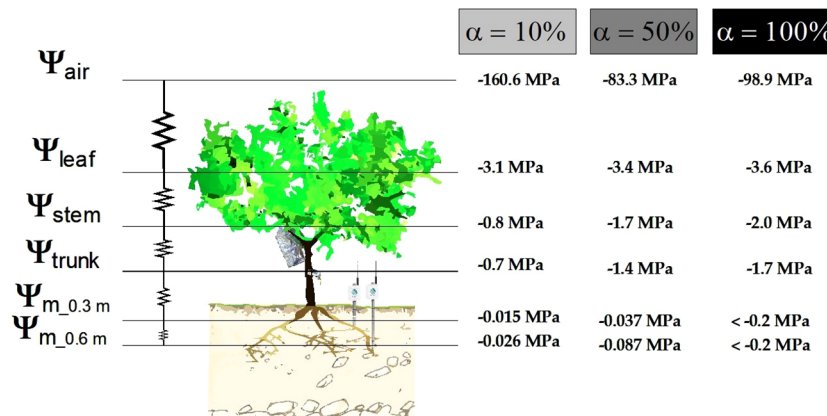


FIGURE 7
 Mean values of water potential at midday in the SPAC during each irrigation criterion: $\alpha=10\%$ (well-irrigated), $\alpha=50\%$ (moderate water deficit), and $\alpha=100\%$ (severe water deficit, non-irrigated).

drip-irrigated nectarine trees. Measurements of Ψ_{trunk} have validated the established MAD-based irrigation protocols (Figure 1B), becoming useful alternative to discrete measurements of leaf or stem water potentials with traditional pressure chamber (Figures 2B, 6). Moreover, Ψ_{trunk} has the advantage of being measured continuously and in real-time, which could lead to automation, whereas Ψ_{leaf} or Ψ_{stem} are destructive, labour-demanding and time-point measurements (Lakso et al., 2022). Nowadays, the information related to the use of Ψ_{trunk} for irrigation management purposes is scarce, and the few available studies deal with irrigation scheduling based on farmer experience (Pagay, 2022) or ETc requirements (Blanco and Kalcsits, 2021).

In our experiment, automated irrigation, based on MAD threshold values fed by real-time θ_v measurements with capacitance probes, has been successfully implemented for drip-irrigated nectarine trees grown in a semi-arid Mediterranean environment. As confirmed in previous studies, significantly higher water, energy and labour savings were achieved using this MAD-based irrigation protocol compared to conventional irrigation scheduling based on calculated crop evapotranspiration (ETc), not only without penalising yield but also improving nectarine fruit quality (Conesa et al., 2019; Conesa et al., 2021; Vera et al., 2019; Vera et al., 2021). In this field experiment, a quite different postulate was applied, in which MAD were managed to reach different soil water deficit conditions, and thus

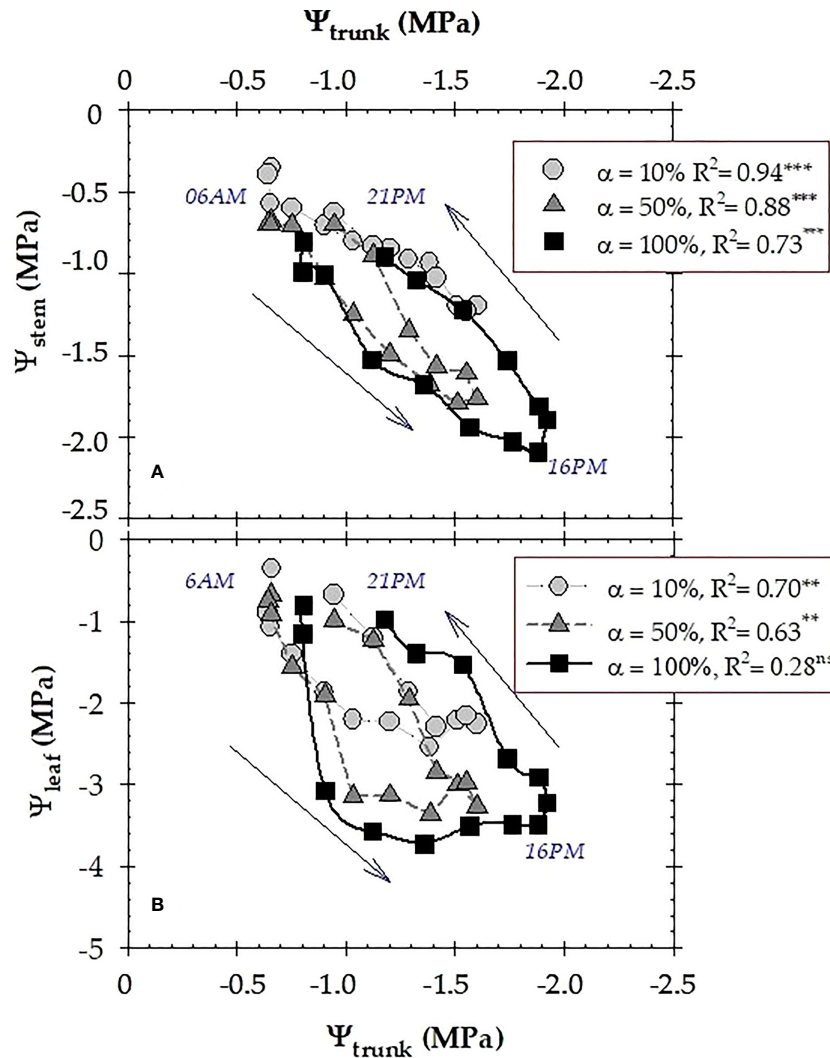


FIGURE 8
 Daily time-course of the relationship between trunk water potential (Ψ_{trunk}) and: **(A)** stem water potential (Ψ_{stem}) and **(B)** leaf water potential (Ψ_{leaf}) at each irrigation criterion: 10% (well-irrigated), 50% (moderate water deficit) and 100% (severe water deficit, non-irrigated), respectively. The data point is the mean of four leaves. R^2 is the coefficient of determination of the linear regression. **: $p \leq 0.01$; ***: $p \leq 0.001$, ns: not significant.

θ_v in the active root zone (0-0.5 m) were remained close to FC values during the first period ($\alpha=10\%$), decreased to 21.5% during $\alpha=50\%$ period, and barely reached 17% at the end of the withholding irrigation period ($\alpha=100\%$). These θ_v values were indicative of well-irrigated, mild and severe soil water deficit conditions, respectively (Figure 1B). Since θ_v sets the upper/lower interval of the available soil water, θ_v variations were due not only in response to irrigation or rainfall events, but also to root water uptake dynamics and, to a lesser extent, diurnal environmental changes. In fact, θ_v dynamics had been closely related to evapotranspiration demand, confirming the sensitivity of capacitance sensors to the nearby environment of soil and plant roots (Mira-García et al., 2021).

Water potentials in the soil-plant-atmosphere continuum (SPAC) provide a physical basis for a comparable quantification of water status. During the summer in the northern hemisphere, the agrometeorological measurements were typical of Mediterranean semi-arid climates (Lionello et al., 2023). Of these, air water

potential (Ψ_a) was calculated as an environmental indicator (Figure 2A), behaving similarly to VPD (Figure 1A), showing a higher day-to-day variability. However, Ψ_a gives an indication of the water potential allowing water flow along the soil-plant path.

Soil water status, estimated by soil matric potential (Ψ_m), also correlated with the irrigation protocol applied (Figure 1B). However, under non-irrigated conditions ($\alpha=100\%$), the soil sensors reached their maximum allowed reading (-200 kPa), which mirrored a significant limitation of these soil water sensors under severe water stress conditions (Figure 2C). Thompson et al. (2006) reported the best performance of these granular matrix sensors when used in wet soil (-10 to -50 kPa). Also, the pattern of Ψ_m at both soil depths (0.3 and 0.6 m) remained almost constant during the daily courses studied (Figures 6G-I), highlighting the drawback of these soil water sensors in identifying diurnal changes because of root water uptake.

Plant water potentials understandably reflected the MAD-based irrigation criteria, evaporative demand and radiation changes that

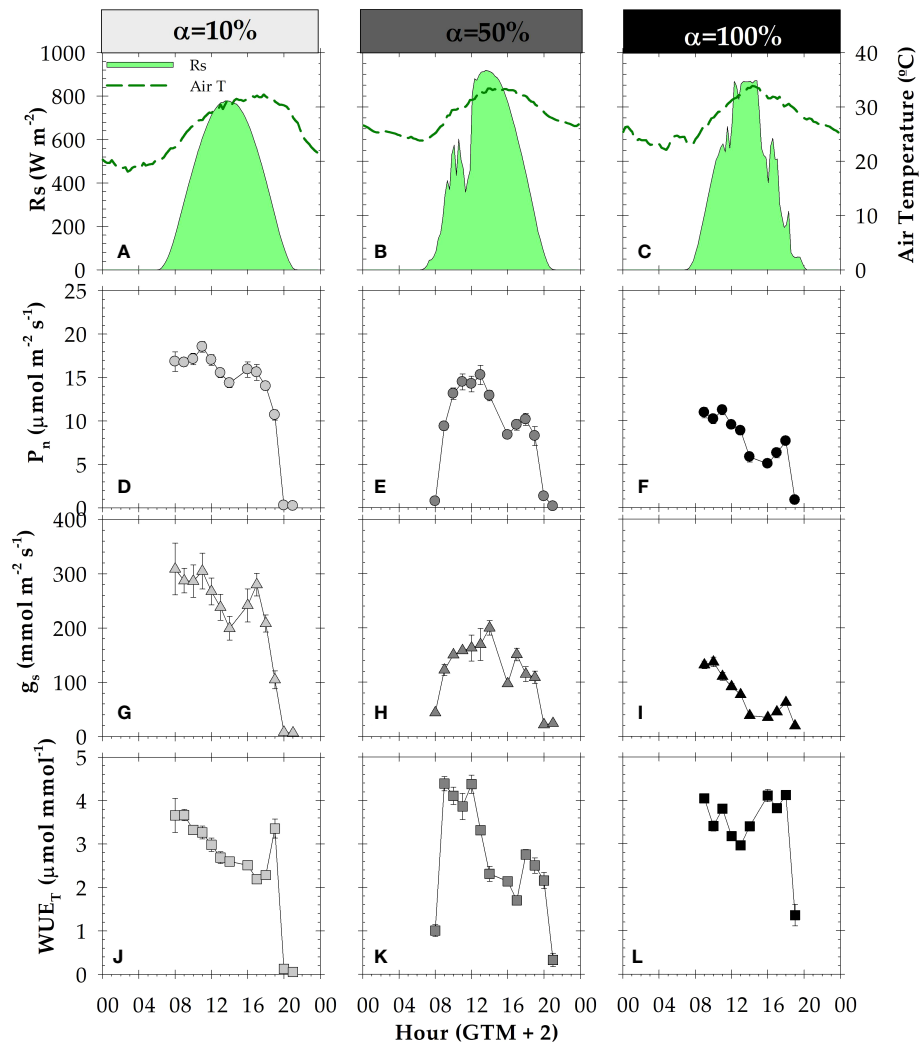


FIGURE 9
 Daily courses of: (A–C) solar radiation (R_s) and air temperature; (D–F) net photosynthesis (P_n); (G–I) stomatal conductance (g_s); (J–L) transpiration efficiency (WUE_T), during different irrigation criteria: $\alpha=10\%$ (DOY 174), $\alpha=50\%$ (DOY 210) and $\alpha=100\%$ (DOY 244). Each point is the mean of four leaves. Vertical bars in data points are \pm SE (not shown when smaller than the symbols). GMT: Greenwich mean time.

occurred throughout the day (Figures 2B, 6D–F). The values of Ψ_{leaf} measured at predawn during the diurnal courses, which decreased as stress accumulated (from -0.35 to -0.8 MPa) (Figures 6D–F), agreed with those obtained in deficit irrigated peach trees by Girona et al. (1993). This valued plant-based measurement, taken at night when there is little or no transpiration, gives an indication of the integrated water status of the soil around the roots (Schmidt and Gaudin et al., 2017), based on the idea that when the plant does not transpire, there is a balance between soil and plant water status. However, there can be erroneous values if there are large variations in soil water levels within the profile (Améglio et al., 1999).

The values of Ψ_{leaf} showed the highest variability of the plant water potentials studied (Figures 2B, 6D–F). This is because it is determined on non-cover sunlit leaves, highly dependent upon leaf conductance values and evaporative demand conditions existing at the time of the measurements (García-Tejara et al., 2021). In this sense, Ruiz-Sánchez et al. (2000) found a strong relationship between leaf insertion angle (LIA) and Ψ_{leaf} in apricot trees, so that the variability in Ψ_{leaf} caused by changes in leaf orientation

allows a lower incidence of solar radiation, and a reduction in water loss and leaf heating (Sánchez-Blanco et al., 1994), which makes sunny leaves sensitive to the time of sun exposure. Consequently, Ψ_{stem} , measured on covered leaves, is considered the standard measure to determine tree water status in fruit trees (Shackel et al., 1997). Since leaf transpiration is prevented, the Ψ_{stem} roughly represents soil water status, and behaved more stable than Ψ_{leaf} (Figures 2B, 6D–F).

In the present study, both Ψ_{trunk} and Ψ_{stem} were strongly correlated ($R^2 = 0.86$, $p < 0.001$), as they provided similar data of plant water path (Figure 4A). Blanco and Kalcsits (2021) found similar correlations with a coefficient of determination up to 0.8 in pear trees. However, the relationship between Ψ_{trunk} vs. Ψ_{leaf} was not significant, highlighting the higher Ψ_{leaf} variability and the weakness of this indicator of plant water status (Figure 4B).

Seasonal values of Ψ_{stem} and Ψ_{trunk} averaged -0.83 and -0.73 MPa, respectively, during the period of $\alpha=10\%$ (Figure 2B), coinciding with the postharvest period in nectarine trees. These values corresponded to non-limiting soil water conditions (Naor et al., 2005; Abrisqueta

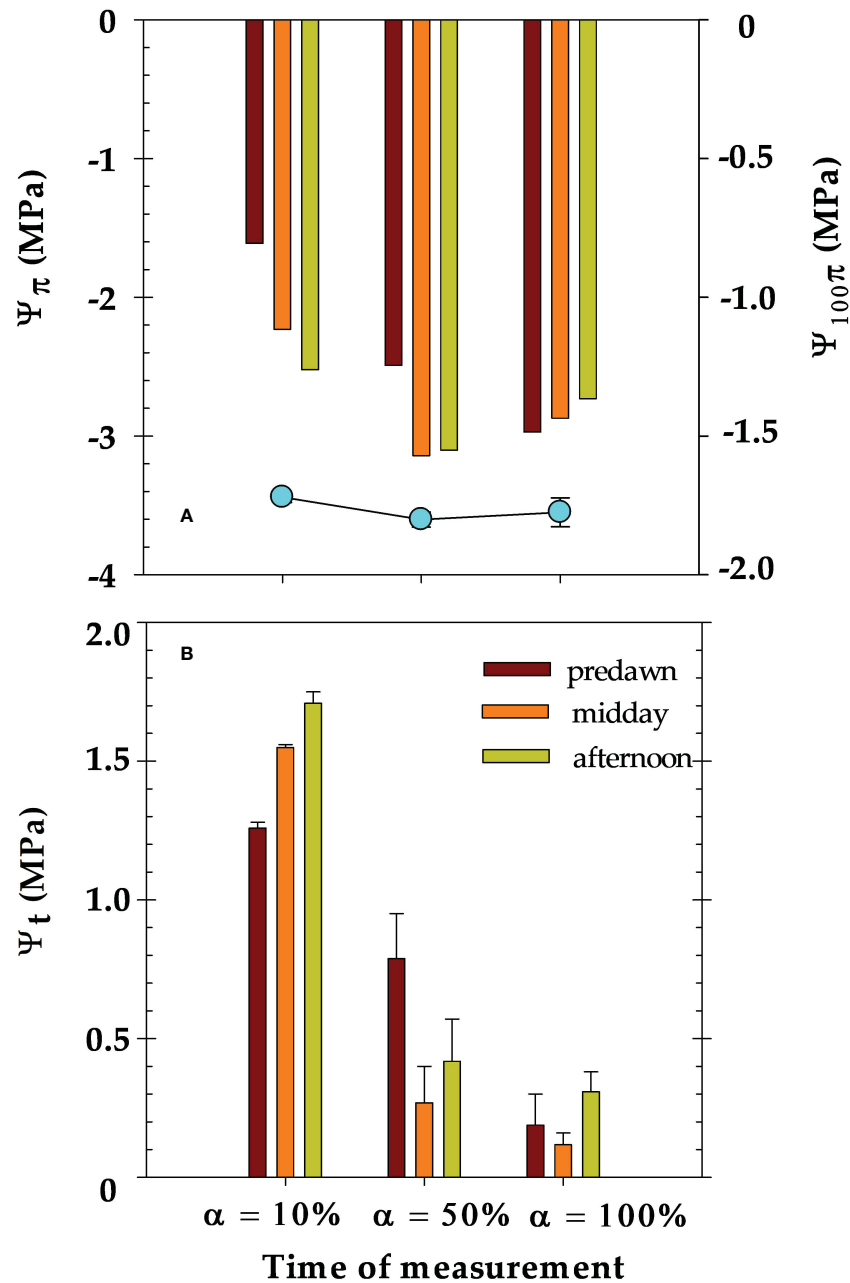


FIGURE 10
 Values of: (A) actual osmotic water potential (Ψ_{π}), and osmotic water potential at full turgor ($\Psi_{\pi 100}$), and (B) leaf turgor potential (Ψ_t) at different times of the day (predawn, midday and afternoon) during the different irrigation criteria: $\alpha=10\%$ (DOY 174), $\alpha=50\%$ (DOY 210) and $\alpha=100\%$ (DOY 244). The measurements were made on the same leaves used for leaf water potential. Each bar is the mean of four leaves \pm ES.

et al., 2015; De la Rosa et al., 2016; Conesa et al., 2019; Vera et al., 2019, Conesa et al., 2021). As expected, the minimum values of Ψ_{stem} (-2.04 MPa) and Ψ_{trunk} (-1.74 MPa) were observed at the end of the non-irrigation period ($\alpha=100\%$) (Figure 2B). Blanco and Kalcits (2021) reported that MTs can accurately assess plant water status within the range of -0.2 to -2.1 MPa of Ψ_{trunk} values in pear trees. Our findings showed a mean gradient of 0.3 MPa between Ψ_{stem} and Ψ_{trunk} (Figures 2B, 6D–F, 7), with slight differences during the experiment. Also, the gradient between Ψ_{leaf} and Ψ_{trunk} was higher than that between Ψ_{stem} and Ψ_{trunk} (mean values of \approx 1.8 MPa), indicative of the high hydraulic resistance between trunk and leaves (Pagay, 2022).

It is noteworthy that when seasonal data of plant and soil water potentials were correlated, the most significant relationship was detected between Ψ_m vs. Ψ_{trunk} ($R^2 = 0.79, p < 0.01$) followed by Ψ_m vs. Ψ_{stem} ($R^2 = 0.62, p < 0.05$) and it was not significant for Ψ_m vs. Ψ_{leaf} ($R^2 = 0.26, p > 0.05$) (Figure 3). Thus, it reveals that Ψ_{trunk} is arguably the most stable indicator of the plant water status, integrating canopy leaves into a stable tissue relatively unaffected by external factors (Lakso et al., 2022; Pagay, 2022).

Leaf gas exchange was also sensitive to MAD-based irrigation criteria (Figure 5). As expected, P_n and g_s decreased during the experiment as water deficit accumulated, suggesting a limitation in photosynthetic capacity under water stress condition (Wong et al.,

TABLE 1 Sensitivity analysis (SI: Signal intensity; CV: coefficient of variation; S: sensitivity (by Goldhamer and Fereres, 2001); and S*: corrected sensitivity (by De la Rosa et al., 2014) for the indicators of plant water status during the experimental period.

Plant water status indicator	SI	CV	S	S*
Ψ_{stem}	2.13	2.15	0.99	1.67
Ψ_{leaf}	1.37	5.01	0.27	1.17
Ψ_{trunk}	2.54	2.47	1.03	2.13
P_n	0.54	2.83	0.19	0.18
g_s	0.39	1.84	0.21	-0.15
WUE_T	0.8	3.08	0.26	0.26

Ψ_{stem} : midday stem water potential (MPa); Ψ_{leaf} : midday leaf water potential (MPa); Ψ_{trunk} : midday trunk water potential (MPa); P_n : net photosynthesis ($\mu\text{mol m}^{-2} \text{s}^{-1}$); g_s : stomatal conductance ($\text{mmol m}^{-2} \text{s}^{-1}$); WUE_T : transpiration efficiency ($\mu\text{mol mmol}^{-1}$).

1979). Meanwhile, transpiration efficiency (WUE_T) tended to increase (Figure 5C). Stomatal closure (Figure 5B) reduced the amount of H_2O lost per CO_2 assimilated, although, the response of this plant indicator to water stress was decreased by the effect of climatic demand (Figures 5C, 1A). It is also important to note that, despite irrigation recovery, mean values of P_n and g_s at this period were lower than those obtained under early summer well irrigated conditions ($\alpha=10\%$). The absence of a full recovery of leaf gas exchange values was motivated by the initiation of leaf senescence typical of deciduous fruit trees (Andersen and Brodbeck, 1988). Furthermore, Conesa et al. (2022) explained the fact that leaf gas exchange levels of water stressed nectarine trees during late postharvest did not recover previous values, after irrigation was restored, by a decrease in the aspartate amino acid in leaves that affected chloroplasts formation.

The hysteresis phenomenon found in the relationships between the two plant water potentials: Ψ_{trunk} vs. Ψ_{stem} (Figure 8A), which was more noticeable for Ψ_{trunk} vs. Ψ_{leaf} (Figure 8B), was higher for the highest imposed soil water deficit ($\alpha=100\%$). This hysteretic behaviour revealed that the water status of the trunk assumes a dominant role in controlling canopy water status as water stress accumulates, which is related to plant hydraulic conductivity during the daily course (Assouline, 2021). In addition, stomata reopened in the afternoon, as indicated by the recovery values of the diurnal pattern of leaf gas exchange (Figures 9G–I).

No osmotic adjustment was observed in leaves of nectarine trees in response to the applied soil water deficit (Figure 10A). In this regard, Mellisho et al. (2011) in peach trees, and Torrecillas et al. (1999) in apricot trees reported the need to reach Ψ_{leaf} and Ψ_{stem} below -2.6 and -2.0 MPa, respectively, to activate this tolerance mechanism. Furthermore, it was observed that leaf turgor (Ψ_t) was maintained, even at $\alpha=100\%$ (Figure 10A). In this sense, other drought tolerance characteristics could have taken place, such as high relative apoplastic water content, which would contribute to water retention at low leaf water potentials (Rodríguez et al., 2012).

It is important to note that Ψ_{trunk} values showed the highest signal intensity and sensitivity values for the plant-based water status indicators studied, followed by Ψ_{stem} (Table 1). These results emphasise that although Ψ_{trunk} had a higher variability (CV) than Ψ_{stem} , it can accurately assess plant water status. Indeed, the S* method (De la Rosa et al., 2014), which decreased the influence of CV in the analysis, showed an increased sensitivity of Ψ_{trunk} . In the same cultivar, Ψ_{stem} and canopy to air temperature difference values

recorded the highest signal intensity and the Normalised Difference Vegetation Index the highest sensitivity for detecting moderate water deficit situations by mid-July (Conesa et al., 2019).

5 Conclusions

Continuous measurements of trunk water potential (Ψ_{trunk}) using microtensiometers, embedded in the tree trunk, agreed with the automated soil MAD-based irrigation protocols applied to a nectarine orchard. Changes in Ψ_{trunk} explained 79% of the soil matric potential. In fact, Ψ_{trunk} was strongly related to discrete determinations of Ψ_{stem} measured with a pressure chamber. A mean gradient of 0.3 MPa was observed between Ψ_{trunk} vs. Ψ_{stem} , and 1.8 MPa between Ψ_{trunk} vs. Ψ_{leaf} . The greatest variability was found in Ψ_{leaf} , due to its dependence on stomatal aperture and evaporative demand conditions. Regarding environmental variables, Ψ_{air} showed a high day-to-day variability and a similar dynamic to VPD. Therefore, Ψ_{air} could be used in water relations studies in the same terms of water potential as in soil and plant.

Considering that real-time Ψ_{trunk} data allows for automation, further research is needed to determine Ψ_{trunk} threshold values for a successful irrigation decision support system. In addition, the stability, and the long-term performance of trunk microtensiometers needs to be tested.

The promising results found in this work point to the potential use of trunk microtensiometers as novel biosensors to accurately real-time monitor plant water status, and eventually served for precise irrigation scheduling.

Data availability statement

The raw data supporting the conclusions of this article will be made available by the authors, without undue reservation.

Author contributions

Study conception and design were performed by MC, JV and MR-S. Formal analysis and data curation by WC and MC. Software and validation by JV and WC. Project administration and funding

acquisition by MR-S. The first draft of the manuscript was written by MC. All authors contributed to the article and approved the submitted version.

Funding

This study was supported by the Spanish State Research Agency [PID2019-106226RB-C2 1/AEI/10.13039/501100011033].

Acknowledgments

MC thanks to the Spanish Juan de la Cierva postdoctoral programme (FJCI-2017-32045 and IJC2020-045450-I) funded by MCIN/AEI/10.13039/501100011033 and European Union NextGenerationEU/PRTR.

References

- Abriquetta, I., Conejero, W., López-Martínez, L., Vera, J., and Ruiz-Sánchez, M. C. (2017). Root and aerial growth in early-maturing peach trees under two crop load treatments. *Span. J. Agric. Res.* 15, e0803. doi: 10.5424/sjar/2017152-10714
- Abriquetta, I., Conejero, W., Valdés-Vela, M., Vera, J., Ortuño, M. F., and Ruiz-Sánchez, M. C. (2015). Stem water potential estimation of drip-irrigated early-maturing peach trees under Mediterranean conditions. *Comp. Electron. Agric.* 114, 7–13. doi: 10.1016/j.compag.2015.03.004
- Allen, R. G., Pereira, J. S., Raes, D., and Smith, M. (1998). *Crop evapotranspiration: guidelines for computing crop water requirements* Vol. 56 (Rome (Italy): FAO), 300.
- Améglio, T., Archerd, P., Cohen, M., Valancogne, C., Audet, F. A., Dayau, S., et al. (1999). Significance and limits in the use of predawn leaf water potential for tree irrigation. *Plant Soil* 207, 155–167. doi: 10.10123/A:1026415302759
- Andersen, P. C., and Brodbeck, B. V. (1988). Water relations and net CO₂ assimilation of peach leaves of different ages. *J. Am. Soc. Hortic. Sci.* 113, 242–248. doi: 10.21273/jashs.113.2.242
- Assouline, S. (2021). What can we learn from the water retention characteristic of a soil regarding its hydrological and agricultural functions? review and analysis of actual knowledge. *Water Res. Res.* 57, e2021WR031026. doi: 10.1029/2021WR031026
- Black, W. L., Santiago, M., Zhu, S. Y., and Stroock, A. D. (2020). Ex situ and in situ measurement of water activity with a MEMS tensiometer. *Anal. Chem.* 92, 716–723. doi: 10.1021/acs.analchem.9b02647
- Blanco, V., and Kalcits, L. (2021). Microtensiometers accurately measure stem water potential. *Plants* 10, 2780. doi: 10.3390/plants10122780
- Burt, C. M., and Styles, S. W. (2007). *Drip and micro irrigation design and management* (CA: ITRC), 396.
- Casadesús, J., Mata, M., Marsal, J., and Girona, J. (2012). A general algorithm for automated scheduling of drip irrigation in tree crops. *Comp. Elect. Agric.* 83, 11–20. doi: 10.1016/j.compag.2012.01.005
- Conesa, M. R., Conejero, W., Vera, J., Agulló, V., García-Viguera, C., and Ruiz-Sánchez, M. C. (2021). Irrigation management practices in nectarine fruit quality at harvest and after cold storage. *Agric. Water Manage.* 243, 106519. doi: 10.1016/j.agwat.2020.106519
- Conesa, M. R., Conejero, W., Vera, J., Ramírez-Cuesta, J. M., and Ruiz-Sánchez, M. C. (2019). Terrestrial and remote indexes to assess moderate deficit irrigation in early-maturing nectarine trees. *Agronomy* 9 (10), 630. doi: 10.3390/agronomy9100630
- Conesa, M. R., Conejero, W., Vera, J., and Ruiz-Sánchez, M. C. (2022). Root reserves ascertain postharvest sensitivity to water deficit of nectarine trees. *Agronomy* 12, 1805. doi: 10.3390/agronomy12081805
- De la Rosa, J. M., Conesa, M. R., Domingo, R., Aguayo, E., Falagán, E., and Pérez-Pastor, A. (2016). Combined effects of deficit irrigation and crop level on early nectarine trees. *Agric. Water Manage.* 170, 120–132. doi: 10.1016/j.agwat.2016.01.012
- De la Rosa, J. M., Conesa, M. R., Domingo, R., and Pérez-Pastor, A. (2014). A new approach to ascertain the sensitivity to water stress of different plant water indicators in extra-early nectarine trees. *Sci. Hortic.* 169, 147–153. doi: 10.1016/j.scienta.2014.02.021
- Dix, M. J., and Aubrey, D. P. (2021). Recalibrating best practices, challenges, and limitations of estimating tree transpiration via sap flow. *Curr. Forestry Rep.* 7, 31–37. doi: 10.1007/s40725-021-00134-x
- FAO (2021). *The state of food security and nutrition in the world (SOFI)* (Rome (Italy): FAO), 240, ISBN:
- FAOSTAT (2022) *Food and agriculture organization statistical data*. Available at: <http://www.fao.org/faostat/en/#data/QC> (Accessed 7 October 2022).
- Fereres, E., and Soriano, M. A. (2007). Deficit irrigation for reducing agricultural water use. *J. Exp. Bot.* 58, 147–159. doi: 10.1093/jxb/erl165
- Fernández, J. E. (2014). Plant-based sensing to monitor water stress: Applicability to commercial orchards. *Agric. Water Manage.* 142, 99–109. doi: 10.1016/j.agwat.2014.04.017
- Fernández, J. E., and Cuevas, M. V. (2010). Irrigation scheduling from stem diameter variations: A review. *Agric. For. Meteorol.* 150, 135–151. doi: 10.1016/j.agrformet.2009.11.006
- Fernández-García, I., Lecina, S., Ruiz-Sánchez, M. C., Vera, J., Conejero, W., Conesa, M. R., et al. (2020). Trends and challenges in irrigation scheduling in the semi-arid area of Spain. *Water* 12, 785. doi: 10.3390/w12030785
- García-Tejara, O., López-Bernal, A., Orgaz, F., Testi, L., and Villalobos, F. J. (2021). The pitfalls of water potential for irrigation scheduling. *Agric. Water Manage.* 243, 106522. doi: 10.1016/j.agwat.2020.106522
- Girona, J., Mata, M., Goldhamer, D. A., Johnson, R. S., and DeJong, T. M. (1993). Patterns of soil and tree water status and leaf functioning during regulated deficit irrigation scheduling in peach. *J. Am. Soc. Hortic. Sci.* 118, 580–586. doi: 10.21273/jashs.118.5.580
- Goldhamer, D. A., and Fereres, E. (2001). Irrigation scheduling protocols using continuously recorded trunk diameter measurements. *Irrig. Sci.* 20, 115–125. doi: 10.1007/s002710000034
- Gucci, R., Xiloyannis, C., and Flores, J. A. (1991). Gas exchange parameters: water relations and carbohydrate partitioning in leaves of field-grown *Prunus domestica* following fruit removal. *Physiol. Plant* 83, 497–505. doi: 10.1111/j.1399-3054.1991.tb00126.x
- Jones, H. G. (2004). Irrigation scheduling: advantages and pitfalls of plant-based methods. *J. Exp. Bot.* 55, 2427–2436. doi: 10.1093/jxb/erh213
- Katerji, N., Mastroilli, M., and Rana, G. (2008). Water use efficiency of crops cultivated in the Mediterranean regions: Review and analysis. *Europ. J. Agron.* 28 (4), 493–507. doi: 10.1016/j.eja.2007.12.003
- Lakso, A. M., Zhu, A., Santiago, M., Shackel, V., Volkov, A., and Stroock, A. D. (2022). “A microtensiometer sensor to continuously monitor stem water potentials in woody plants—design and field testing,” in *Proc. IX int. symp. on irrigation of horticultural crops*, vol. 1335. Ed. C. Xiloyannis, et al (Acta Hortic), 317–324. doi: 10.17660/ActaHortic.2022.133.39
- Lionello, P., Giorgi, F., Rohling, E., and Seager, R. (2023). “Chapter 3. Mediterranean climate: past, present and future,” in *Oceanography of the Mediterranean Sea*. Eds. K. Schroeder and J. Chiggiato (Elsevier), 41–91, ISBN: . doi: 10.1016/B978-0-12-823692-5.00011-X
- Martínez-Gimeno, M. A., Castiella, M., Rügler, S., Intrigliolo, D. S., and Ballester, C. (2017). Evaluating the usefulness of continuous leaf turgor pressure measurements for the assessment of persimmon tree water status. *Irrig. Sci.* 35, 159–167. doi: 10.1007/s00271-016-0527-3
- McCutchan, H., and Shackel, K. A. (1992). Stem water potential as a sensitive indicator of water stress in prune trees (*Prunus domestica* L. cv. French). *J. Am. Soc. Hortic. Sci.* 177, 607–611. doi: 10.21273/jashs.117.4.607
- Mellisho, C. D., Cruz, N. Z., Conejero, W., Ortuño, M. F., and Rodríguez, P. (2011). Mechanisms for drought resistance in early maturing cv. flordastar peach trees. *J. Agric. Sci.* 149, 609–616. doi: 10.1017/S0021859611000141

Conflict of interest

The authors declare that the research was conducted in the absence of any commercial or financial relationships that could be construed as a potential conflict of interest.

Publisher's note

All claims expressed in this article are solely those of the authors and do not necessarily represent those of their affiliated organizations, or those of the publisher, the editors and the reviewers. Any product that may be evaluated in this article, or claim that may be made by its manufacturer, is not guaranteed or endorsed by the publisher.

- Merriam, J. L. (1966). A management control concept for determining the economical depth and frequency of irrigation. *Trans. ASAE* 9, 492–498. doi: 10.13031/2013.40014
- Millán, S., Casadesús, J., Campillo, C., Moñino, M. J., and Prieto, M. H. (2019). Using soil moisture sensors for automated irrigation scheduling in a plum crop. *Water* 11, e2061. doi: 10.3390/w11102061
- Mira-García, A. B., Vera, J., Conejero, W., Conesa, M. R., and Ruiz-Sánchez, M. C. (2021). Evapotranspiration in young lime trees with automated irrigation. *Sci. Hort.* 288, 110396. doi: 10.1016/j.scienta.2021.110396
- Naor, A., Stern, R., Peres, M., Greenblat, Y., Gal, Y., and Flaishman, M. A. (2005). Timing and severity of postharvest water stress affect following year productivity and fruit quality of field-grown 'Snow queen' nectarine. *J. Amer. Soc. Hort. Sci.* 130, 806–812. doi: 10.21273/jashs.130.6.806
- Navarro, A., Portillo-Estrada, M., and Ceulemans, R. (2020). Identifying the best plant water status indicator for bio-energy poplar genotypes. *GCB Bioenergy* 12, 426–444. doi: 10.1111/gcbb.12687
- Nobel, P. (1983). *Biophysical plant physiology and ecology* (New York, USA: W.H. Freeman and Company), 608.
- Ortuño, M. F., Conejero, W., Moreno, F., Moriana, A., Intrigliolo, D. S., Biel, C., et al. (2010). Could trunk diameter sensors be used in woody crops for irrigation scheduling? a review of current knowledge and future perspectives. *Agric. Water Manage.* 97, 1–11. doi: 10.1016/j.agwat.2009.09.008
- Osroosh, Y., Peters, R. T., Campbell, C. S., and Zhang, Q. (2016). Comparison of irrigation automation algorithms for drip-irrigated apple trees. *Comp. Elect. Agric.* 128, 87–99. doi: 10.1016/j.compag.2016.08.013
- Padilla-Díaz, C. M., Rodríguez-Domínguez, C. M., Pérez-Martín, A., Montero, A., García, J. M., and Fernández, J. E. (2018). Scheduling a deficit irrigation strategy from leaf turgor measurements: Impact on water status, gas exchange and oil yield. *Acta Hort.* 1199, 267–272. doi: 10.17660/ActaHortic.2018.1199.41
- Pagay, V. (2022). Evaluating a novel microtensiometer for continuous trunk water potential measurements in field-grown irrigated grapevines. *Irrig. Sci.* 40, 45–54. doi: 10.1007/s00271-021-00758-8
- Pagay, V., Santiago, M., Sessoms, D. A., Huber, W. J., Vincent, O., Pharkya, A., et al. (2014). A microtensiometer capable of measuring water potential below -10 MPa. *Lab. Chip* 14, 2806–2817. doi: 10.1039/c4lc00342j
- Rodríguez, P., Mellisho, C. D., Conejero, W., Cruz, Z. N., Ortuño, M. F., Galindo, A., et al. (2012). Plant water relations of leaves of pomegranate trees under different irrigation conditions. *Environ. Exp. Botany* 77, 19–24. doi: 10.1016/j.envexpbot.2011.08.018
- Romero, R., Muriel, J. L., García, I., and Muñoz-de la Peña, D. (2012). Research on automatic irrigation control: State of the art and recent results. *Agric. Water Manage.* 114, 59–66. doi: 10.1016/j.agwat.2012.06.026
- Ruiz-Sánchez, M. C., Domingo, R., and Castel, J. R. (2010). Review. deficit irrigation in fruit trees and vines in Spain. *Span. J. Agric. Res.* 8 (S2), 5–20. doi: 10.5424/sjar/201008s2-1343
- Ruiz-Sánchez, M. C., Domingo, R., Torrecillas, A., and Pérez-Pastor, A. (2000). Water stress preconditioning to improve drought resistance in young apricot plants. *Plant Sci.* 156, 245–225. doi: 10.1111/j.1744-7348.1999.tb00883.x
- Sánchez-Blanco, M. J., Alarcón, J. J., Planes, A., and Torrecillas, A. (1994). Differential flood stress resistance of two almond cultivars based on survival, growth and water relations as stress indicators. *J. Hort. Sci.* 69, 947–953. doi: 10.1080/14620316.1994.11516531
- Schmidt, J. E., and Gaudin, A. M. C. (2017). Toward an integrated root ideotype for irrigated systems. *Trends in Plant Science* 22 (5), 433–443. doi: 10.1016/j.tplants.2017.02.001
- Shackel, K. A., Ahmadi, H., Biasi, W., Buchner, R., Goldhamer, D., Gurusinghe, S., et al. (1997). Plant water status as an index of irrigation need in deciduous fruit trees. *HortTechnology* 7 (1), 23–29. doi: 10.21273/HORTTECH.7.1.23
- Smith, D. H., and Allen, S. J. (1996). Measurement of sap flow in plant stems. *J. Exp. Bot.* 47 (12), 1833–1844. doi: 10.1093/jxb/47.12.1833
- Starr, J. L., and Paltineanu, I. C. (2002). "Capacitance devices," in *Methods of soil analysis. part 4 physical methods*. Eds. J. H. Dane and G. C. Topp (Madison, Wisconsin, USA), 463–474.
- Thompson, R. B., Gallardo, M., Aguilera, T., Valdez, L. C., and Fernández, M. D. (2006). Evaluation of watermark sensor for use with drip irrigated vegetable crops. *Irrig. Sci.* 24, 185–200. doi: 10.1007/s00271-005-0009-5
- Torrecillas, A., Galego, R., Pérez-Pastor, A., and Ruiz-Sánchez, M. C. (1999). Gas exchange and water relations of young apricot plants under drought conditions. *J. Agric. Sci.* 132, 445–452. doi: 10.1017/s0021859699006577
- Turner, N. C. (1988). Measurement of plant water status by the pressure technique. *Irrig. Sci.* 9, 289–308. doi: 10.1007/BF00296704
- Varela-Ortega, C., Blanco-Gutiérrez, I., Esteve, P., Bharwani, S., Fronzek, S., and Downing, T. E. (2016). How can irrigated agriculture adapt to climate change? insights from the guadiana basin in Spain. *Reg. Environ. Change* 16, 59–70. doi: 10.1007/s10113-014-0720-y
- Vera, J., Abrisqueta, I., Conejero, W., and Ruiz-Sánchez, M. C. (2017). Precise sustainable irrigation: A review of soil-plant-atmosphere monitoring. *Acta Hort.* 1150, 195–200. doi: 10.17660/ActaHortic.2017.1150.28
- Vera, J., Conejero, W., Conesa, M. R., and Ruiz-Sánchez, M. C. (2019). Irrigation factor approach based on soil water content: A nectarine orchard case study. *Water* 11, 589. doi: 10.3390/w11030589
- Vera, J., Conejero, W., Mira-García, A. B., Conesa, M. R., and Ruiz-Sánchez, M. C. (2021). Towards irrigation automation based on dielectric soil sensors. *J. Hort. Sci. Biotech.* 96 (6), 696–707. doi: 10.1080/14620316.2021.1906761
- Vera, J., and de la Peña, J. M. (1994). *FERTIGA: Programa de fertirrigación de frutales* (Murcia, Spain: CEBAS-CSIC), 69.
- Vories, E., and Sudduth, K. (2021). Determining sensor-based field capacity for irrigation scheduling. *Agric. Water Manage.* 250, 106860. doi: 10.1016/j.agwat.2021.106860
- Wong, S. C., Cowan, I. R., and Farquhar, G. D. (1979). Stomatal conductance correlates with photosynthetic capacity. *Nature* 282, 424–426. doi: 10.1038/282424a0